Vision-based UAV landing on a moving platform in GPS denied environments using motion prediction

Raul Acuna, Ding Zhang, Volker Willert
IAT
TU Darmstadt
Darmstadt, Germany
(racuna, vwillert)@rmr.tu-darmstadt.de

***Abstract*—In this paper, we propose a vision-based control system which enables a multi-rotor unmanned aerial vehicle (UAV) to track an unmanned ground vehicle (UGV) and land on it by using mainly the input of an integrated vision sensor without external localization systems. Our solution is able to generate and follow agile approaching maneuvers in which the target vehicle may leave the field of view of the UAV's vision sensor. This is particularly relevant in scenarios where external localization systems such as GPS are not available or not reliable. In our approach, the UAV observes the movement of the UGV, predicts its motion and generates a smooth approach trajectory to the predicted position. A 6-DOF controller in cascade form is used to track the trajectory, which can lead to movements were the UGV is lost from the field of view (FOV), and then once the UGV is back on the FOV a normal visual servoing tracking is used for landing. The UAV states required for the control law were obtained from an Extended Kalman Filter in combination with a Mahony complementary filter using only internal sensors. The control law and the landing state machine were implemented in ROS and the simulations were developed on Gazebo based on the Rotors simulator.**

***Index Terms*—UAV, autonomous landing, tracking, visual servoing, motion prediction**

I. Introduction

An unmanned aerial vehicle, commonly known as a UAV, is an aircraft which is able to fly without a human pilot on board. Compared to manned aircraft, UAVs are usually preferred for missions that are considered too dull, repetitive or even dangerous for human pilots [1]. In recent years, plenty of impressive achievements on UAVs were made both in research and commercial applications. However, the development of fully autonomous applications for multicopters with the capability of performing complex missions in cooperation with ground robots is still quite challenging. In those situations, high precision aircraft pose estimation is usually required, especially in taking off and landing phases [2].

The choice of sensors to estimate the UAV position and orientation plays a crucial role. The orientation of a multicopter UAV is usually measured through an Inertial Measurement Unit (IMU) and for outdoors, GPS. However, GPS measurements have low accuracy, which is not enough for high precision tasks such as landing. Moreover, it is not possible to use GPS navigation in indoor applications. As an alternative method a camera may be used, but in order to land on the target, generally, a direct line of sight is needed. Most visual-based landing solutions are based on a visual servoing approach which requires constant target tracking, this limits the movement of the UAV and fixes its dynamics to those of the UGV.

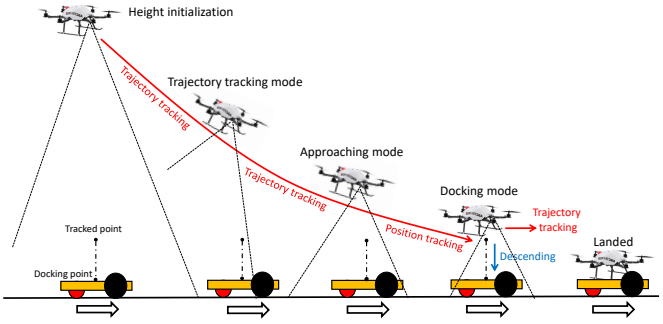

Fig. 1. The state machine of the proposed multicopter landing system.

Our main motivation is to contribute to the current research in this field by developing a more agile strategy based on a control system that enables a UAV to track a mobile unmanned ground vehicle (UGV), predict its position, and dynamically approach and land on it by relying only on relative camera measurements, see Figure 1.

II. Related Literature

A vision-based feedback controller was designed in [1] for autonomous landing of a quadrotor UAV on a floating platform at sea by using an incremental back-stepping control algorithm for the attitude stabilization and position tracking. In [3] a modified back-stepping controller was also used for the attitude stabilization. In [4], a downward-looking camera tracks a target with known characteristics and a template-matching algorithm is used to detect the target in the images and use the detected target pose with a trajectory controller for landing a helicopter.

A system that would allow a UAV to land autonomously on a carrier moving on the ground was presented in [2], the authors employed a Wii remote infrared camera for tracking a known pattern of infrared lights installed in the moving carrier and a PI controller was added to the control loop of the camera to keep it facing towards the carrier.

The authors of [5] provided a trajectory planning and re-planning strategy based on the flatness of the quad-rotor model. An inverse dynamic model of the quad-rotor was derived, whose input is the desired trajectory and output is the control effort actuator.

At the University of Pennsylvania, a controller was designed for aggressive maneuvering of a quad-rotor [6]. The helicopter could perch on a steady inclined surface. This was achieved through a method that allowed the UAV to fly through any position in space with reasonable velocity and pitch (3-D trajectory control). [7] discussed a mobile landing platform for miniature VTOL vehicles. The system consisted of a UGV with a landing platform mounted on top. A gimbaled subsystem design was proposed and the necessary equations were derived to level the platform regardless of the pose of the ground vehicle. This idea was developed for operation on hard surfaces, but can be transferred to a platform on the sea, as shown in [1]. In more recent research, the landing on a moving car was performed by using relative GPS measurements for the long range followed by a visual servoing phase for the final landing [8].

However, in the literature, it is in general not studied what happens if the target is lost from the FOV of the camera. Most research is focused on camera tracking using either image-based visual servoing (IBVS) or position based visual servoing (PBVS) for the close range landing phase and to keep the target on sight usually an actuated Gimbal is used, forcing the restriction of having the target continuously in the field of view which limits the control options and reduce the range of dynamic movements for the UAV. To the best of our knowledge, no methods deal explicitly with the situation of losing the target from the field of view of the camera.

We propose a system in which the UAV dynamically approaches to the UGV once it has been detected, even if by doing so the UGV is lost from the FOV of the bottom camera due to the agile movements. In order to do so, the UGV's movement is tracked and its motion predicted. A reference trajectory is designed which positions the UAV on top of the UGV with the same translational velocities and orientation, this trajectory is then followed without using the reference of the target. At the end of the trajectory, the UAV matches the speed and orientation of the UGV and a regular position based visual servoing approach is used to land.

III. Design Solution

The main goal is to land on a moving vehicle by using relative information obtained from a vision sensor, i.e. a camera. It is assumed that the multirotor has an RGB camera looking straight down plus the regular sensors present on a UAV (regular IMU and odometry sensor such as Pixflow), we assume situations were GPS data is not available or not reliable. The UGV will be tracked using the camera by a fiducial marker attached to the top of the landing platform. We are using as a reference the Asctec Firefly hexacopter with a Pointgrey Blackfly camera and Aruco markers for the tracking of the UGV.

In order to accomplish the landing mission a set of performance goals are defined:

1) We assume that no GPS is available, so the state estimation and tracking of the UGV should be heavily based on the vision sensor.
2) UAV roll and pitch at docking point should be zero, we assume flat surfaces for the UGV and no inclined landing platforms.
3) The heading of the UAV is required to be identical to that of UGV at the docking point.
4) The UAV should land on a UGV that moves along any kind of trajectory, not only linear. Thus a trajectory tracking controller for the position, velocity, and acceleration must be designed.
5) Countermeasures are required for the conditions when loss of target is inevitable, such as a dynamical approach.

Thus a state machine is proposed and developed in order to fulfill those requirements. Figure 1 shows the principle of the state machine diagram with different control modes, this includes all possible states before, during and after the landing process. The state machine is comprised by the following modes:

1) **Observation mode:** The multicopter is initialized hovering above the earth plane, the height of the multicopter is set to a height h, which is defined as the maximum range of the UGV detection using a camera, this height depends on the fiducial used for detection and the camera parameters. The multicopter observes the environment until the the UGV enters its FOV, once the target is available the trajectory tracking mode is activated.
2) **Trajectory generation and tracking mode:**
Two methods are used. The first one defines a smooth trajectory with a cubic spline for all three dimensions of UAV position in N-frame:

$$\boldsymbol{P}(t) = \boldsymbol{P}_0 + 3(\boldsymbol{P}_d - \boldsymbol{P}_0)\frac{t^2}{t_d^2} - 2(\boldsymbol{P}_d - \boldsymbol{P}_0)\frac{t^3}{t_d^3}, \quad (1)$$

where $\boldsymbol{P}_d$ is the desired position setpoint for the UAV, $\boldsymbol{P}_0$ is the current UAV position and t_d is the desired time to reach the setpoint. $\boldsymbol{P}_d$ is defined as the current position of the UGV. The cubic spline trajectory will be updated every iteration as long as the UGV is in the FOV of multicopter, this is the basic approach.
Our improved approach involves the integration of a UGV trajectory prediction algorithm based on curve fitting. The relative position of the UGV is tracked and at least 100 sample points are obtained from the camera measurements of the fiducial marker. Then, a curve fitting algorithm (order 4) is used to predict the future position of the UGV at a given prediction horizon. A setpoint $\boldsymbol{P}_d$ is defined $1\,\mathrm{m}$ right above the target UGV in the predicted position of the UGV. A trajectory is generated to the setpoint and then followed using only information from the odometry sensor and IMU since it is possible to lose the UGV from the field of view of

the camera. After the trajectory tracking is over at time t_d and $\boldsymbol{P}_0 - \boldsymbol{P}_d$ is smaller than a threshold value, the system switches to approaching mode.

3) **Approaching mode:** In this mode, the UAV will be controlled based only on the setpoint and no longer the trajectory. The target UGV will be continuously tracked during approaching mode using a position based visual servoing approach until the error between the setpoint and the UAV position is smaller than a threshold value, (in our case set to 5 cm). The state machine will be then switched to docking mode.
4) **Docking mode:** Once this mode is activated, the UAV is gradually descended with a cubic spline curve while tracking the UGV horizontal position. The motors are then turned off by the docking point.

IV. Multicopter Model

In this section, a mathematical model of the multicopter dynamics will be presented. We follow similar models presented in [1] and [9]. The specifics of our model are based on the characteristics of the AscTec Firefly hexacopter [10]. According to the practice in the field aerospace research, the multicopter UAV is usually considered as a rigid body with 6-DOF as shown in Figure 2, where the earth-fixed and the UAV body-fixed reference coordinate are defined as inertial frame $\{N\}$ and body frame $\{B\}$ respectively. Let $\boldsymbol{R}_b^n$ denote the rotation matrix from $\{B\}$ to $\{N\}$, the multicopter dynamics can be expressed by following equations:

$$\dot{\boldsymbol{P}}_n = \boldsymbol{R}_b^n \boldsymbol{V}_b \tag{2}$$

$$\dot{\boldsymbol{V}}_b = -\boldsymbol{\Omega} \times \boldsymbol{V}_b + m^{-1}(\boldsymbol{G} + \boldsymbol{T}) \tag{3}$$

$$\dot{\boldsymbol{\Theta}} = \boldsymbol{W}\boldsymbol{\Omega} \tag{4}$$

$$\dot{\boldsymbol{\Omega}} = \boldsymbol{J}^{-1}(-\boldsymbol{\Omega} \times \boldsymbol{J}\boldsymbol{\Omega} + \boldsymbol{\tau}_a) \tag{5}$$

Where the system state vectors are denoted as:

- Absolute position in $\{N\}$-frame: $\dot{\boldsymbol{P}}_n = (x_n, y_n, z_n)^T$
- Linear velocity in $\{B\}$-frame: $\boldsymbol{V}_b = (u, v, w)^T$
- Attitude in Euler angles: $\boldsymbol{\Theta} = (\phi, \theta, \psi)^T$
- Angular rates in $\{B\}$-frame: $\boldsymbol{\Omega} = (p, q, r)^T$

And with the forces, rotary moments, inertia and gravity defined as:

- Thrust force of actuation in $\{B\}$-frame: $\boldsymbol{T} = (0, 0, T)^T$
- Moments of actuation in $\{B\}$-frame: $\boldsymbol{\tau_a} = (\tau_1, \tau_2, \tau_3)^T$
- Inertia matrix $\boldsymbol{J}$ in $\{B\}$-frame: $diag\{I_u, I_v, I_w\}$
- Gravity in $\{B\}$-frame: $\boldsymbol{G} = \boldsymbol{R}_n^b \cdot (0, 0, mg)^T$

The 3×3-matrix $\boldsymbol{W}$ is given by:

$$\boldsymbol{W} = \begin{bmatrix} 1 & \sin\phi\tan\theta & \cos\phi\tan\theta \\ 0 & \cos\phi & -\sin\phi \\ 0 & \sin\phi\sec\theta & \cos\phi\sec\theta \end{bmatrix}. \tag{6}$$

$\boldsymbol{W}$ depends only on $\boldsymbol{\Theta}(\phi, \theta, \psi)$, and the $\det(\boldsymbol{W}) = \sec\theta$. Moreover, $\boldsymbol{W}$ is invertible when the pitch angle satisfies $\theta \neq \frac{(2k-1)\pi}{2}$ $(k = 1, 2, 3, \cdots)$ [3]. In the model, the axis of each propeller is assumed parallel to the axis z_b as in Figure 2. Thus the thrust force T_i and the reactive moment $M_{Q,i}$ caused by air drag produced by each single rotor can be expressed as:

$$T_i = k_T \omega_i^2 \tag{7}$$

$$M_{Q,i} = k_M \omega_i^2, \qquad (i = 1, 2, 3, 4, 5, 6) \tag{8}$$

where k_T and k_M denotes the rotary moment coefficient of every single rotor and ω_i denotes the rotary speed of rotor i. Since the motor dynamics are considerably faster than those of the UAV motion, they can be neglected. Thus, the map from the rotor speed vector $(\omega_1, \omega_2, \cdots, \omega_6)^T$ to the input vector of the UAV model $(T, \tau_1, \tau_2, \tau_3)^T$ can be described as a so-called allocation matrix $\mathfrak{A}$ as expressed below:

$$\begin{bmatrix} T \\ \tau_1 \\ \tau_2 \\ \tau_3 \end{bmatrix} = \mathfrak{A} \begin{bmatrix} \omega_1^2 \\ \omega_2^2 \\ \omega_3^2 \\ \omega_4^2 \\ \omega_5^2 \\ \omega_6^2 \end{bmatrix}, \tag{9}$$

with

$$\mathfrak{A} = k_T \begin{bmatrix} 1 & 1 & 1 & 1 & 1 & 1 \\ -ls_{30} & -l & -ls_{30} & ls_{30} & l & ls_{30} \\ -lc_{60} & 0 & -lc_{60} & lc_{60} & 0 & lc_{60} \\ k_M & -k_M & k_M & -k_M & k_M & -k_M \end{bmatrix}, \tag{10}$$

where l denotes the UAV arm length, s_x and c_x stand for $\sin(x)$ and $\cos(x)$ with x expressed in degrees [11].

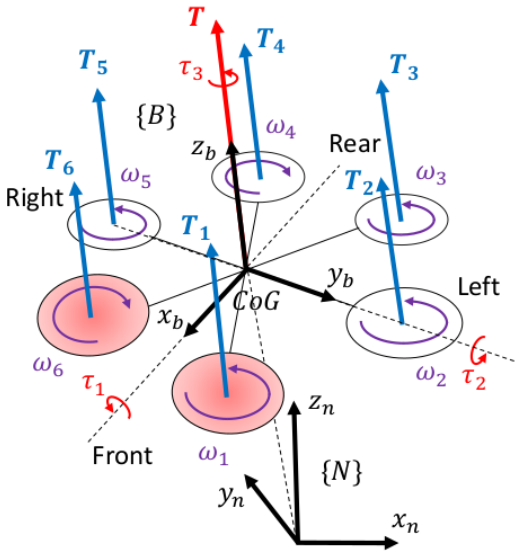

Fig. 2. Dynamic model of a hexacopter and the actuator forces and moments acting on it.

A. State Estimation

An extended Kalman filter (EKF) [12] comprises the main part of the state estimation algorithm as shown in Figure 3.

However, attitude angles derived directly from EKF are not accurate enough, so as a compensation of those drawbacks, a Mahony complementary filter [13] is used to estimate the attitude angles from the IMU measurements.

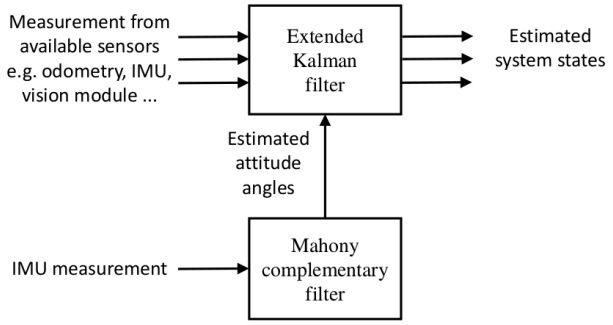

Fig. 3. Block diagram of the implemented state estimation module for the multicopter UAV

V. Control Design

A. Trajectory control methodology

The proposed control structure is presented in Figure 4. The system state machine generates a desired trajectory $\boldsymbol{P}_{n,ref}$ and a heading angle ψ_{ref} for the UAV which are then used as the input of the outer position control loop. The outer loop will generate a desired acceleration vector $\boldsymbol{a}_{n,ref}$. By applying equations (2) to (5), the $\boldsymbol{a}_{n,ref}$ can be easily transformed into the desired thrust T_{ref} and attitude angles $\boldsymbol{\Theta}_{ref}$:

$$\phi_{ref} = \arctan\left(\frac{a_{x,ref}\cos\psi_{ref} + a_{y,ref}\sin\psi_{ref}}{a_{z,ref}+g}\right) \tag{11}$$

$$\theta_{ref} = \arcsin\left(\frac{a_{x,ref}\sin\psi_{ref} - a_{y,ref}\cos\psi_{ref}}{\sqrt{a_{x,ref}^2 + a_{y,ref}^2 + (a_{z,ref}+g)^2}}\right) \tag{12}$$

$$\begin{aligned} T_{ref} = m[&a_{x,ref}(\sin\theta\cos\psi\cos\phi + \sin\psi\cos\phi) + \cdots \\ &+ a_{y,ref}(\sin\theta\sin\psi\cos\phi - \cos\psi\sin\phi) + \cdots \\ &+ (a_{z,ref}+g)\cos\theta\cos\phi], \end{aligned} \tag{13}$$

which are the inputs of the inner attitude control loop. The control methods for outer and inner loops are not unique. Nonlinear controller based on Lyapunov stablization analysis for example ensures the stability and the dynamic behavior of the system, linear PID controller on the other hand is only a approximation for controlling linearized system but with much less complexity. In this work, a hybrid control algorithm with both advantages of nonlinear-backstepping-control and linear PID control is proposed.

B. Outer loop for position control

A continuously differentiable reference trajectory is planned by the prediction algorithm for a time interval in the future $t \in [t_0, t_e]$ as

$$\boldsymbol{P}_{n,ref}(t) = (x_n(t), y_n(t), z_n(t))^T, \tag{14}$$

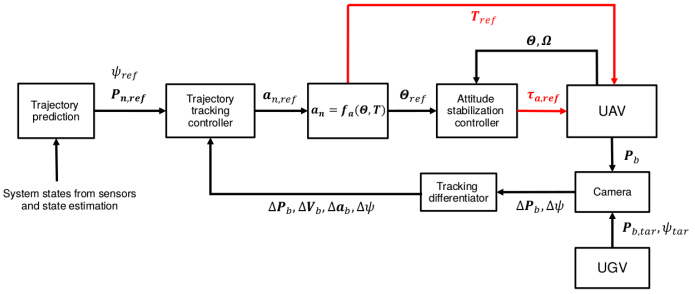

Fig. 4. Structure of the autonomous landing controller with a cascade control structure.

with reference yaw angle $\psi_{ref}(t)$. Then the a PD-control law is used with feed-forward reference acceleration given by

$$\begin{aligned} \boldsymbol{a}_{n,ref} =& \ddot{\boldsymbol{P}}_{n,ref} + \boldsymbol{K}_d(\dot{\boldsymbol{P}}_{n,ref} - \dot{\boldsymbol{P}}_n) \\ &+ \boldsymbol{K}_p(\boldsymbol{P}_{n,ref} - \boldsymbol{P}_n), \end{aligned} \tag{15}$$

where all the time derivatives are acquired via a tracking differentiator.

C. Inner loop for attitude control

Attitude control plays a crucial part for generating the acceleration of the UAV body. A back-stepping algorithm with command filter is implemented for the attitude stabilization control, as described by

$$\boldsymbol{\Omega}_{ref} = \boldsymbol{W}^{-1}(-\boldsymbol{c}_\Theta \boldsymbol{e}_\Theta + \dot{\boldsymbol{\Theta}}_c) \tag{16}$$

$$\boldsymbol{\tau}_{a,ref} = -\boldsymbol{J}\boldsymbol{c}_\Omega \boldsymbol{e}_\Omega + \boldsymbol{\Omega} \times \boldsymbol{J}\boldsymbol{\Omega} - \boldsymbol{W}\bar{\boldsymbol{e}}_\Theta + \boldsymbol{J}\dot{\boldsymbol{\Omega}}_c, \tag{17}$$

with the state error as

$$\bar{\boldsymbol{e}}_\Theta = \boldsymbol{e}_\Theta - \boldsymbol{\chi}_\Theta = \boldsymbol{\Theta} - \boldsymbol{\Theta}_{ref} - \boldsymbol{\chi}_\Theta \tag{18}$$

$$\boldsymbol{e}_\Omega = \boldsymbol{\Omega} - \boldsymbol{\Omega}_{ref}, \tag{19}$$

the command filter dynamic defined by

$$\dot{\boldsymbol{\Theta}}_c = -\boldsymbol{\tau}_{cmd,\Theta}(\boldsymbol{\Theta}_c - \boldsymbol{\Theta}_{ref}) \tag{20}$$

$$\dot{\boldsymbol{\Omega}}_c = -\boldsymbol{\tau}_{cmd,\Omega}(\boldsymbol{\Omega}_c - \boldsymbol{\Omega}_{ref}), \tag{21}$$

and the state error compensating factor dynamic

$$\dot{\boldsymbol{\chi}}_\Theta = -\boldsymbol{c}_\Theta \boldsymbol{\chi}_\Theta + \boldsymbol{W}(\boldsymbol{\Omega}_c - \boldsymbol{\Omega}_{ref}). \tag{22}$$

VI. Experimental Results

The proposed control design was implemented in ROS and simulated in the Gazebo simulator. The 3D simulation model of the UAV is provided by the *rotors_simulator* ROS package [14]. The overall settings of the Gazebo simulation environment as well as the relevant parameters of *rotors_simulator* were configured as follows:

- The sample time of the controller was configured as 1 ms, and the update frequency of the simulated onboard bottom camera as 30 fps with a resolution of 1024×1024 px.
- 2D Aruco fiducial Markers are used for the identification of the UGV landing plattform. The ROS package *ar_sys* has been used for marker detection and relative pose estimation.

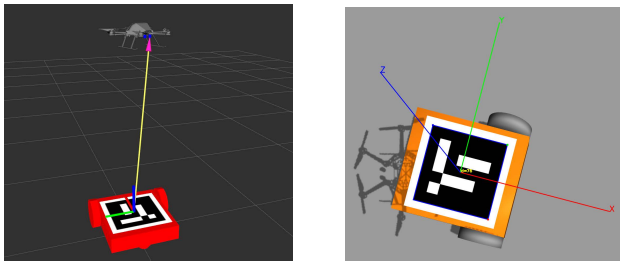

(a) UAV und UGV model (b) On board camera image

Fig. 5. 3D physical models in Gazebo

- The ratio between the noise amplitude and the measured value from the camera signal is set to be 1/50, which means the uncertainty of the position measurements is about $\pm 2\,\mathrm{cm}$.
- The maximum reference value of pitch and roll of the multicopter is set to be $30°$ for security. However if the pitch and roll angle becomes greater than $60°$, then the multicopter is regarded as flipped over, which leads to a emergency shut down behavior of the motors.
- The relevant parameters of the *AscTec* Firefly hexacopter used in the simulation tests are:

$$\boldsymbol{J} = diag\{0.0348, 0.0459, 0.0978\}\ \mathrm{kg\,m^2}, \quad (23)$$

$$m = 1.5\ \mathrm{kg}, \quad (24)$$

$$k_T = 6.7 \times 10^{-6}\ \mathrm{Ns/rad}, \quad (25)$$

$$k_m = 0.0365\ \mathrm{m}, \quad (26)$$

$$0 \leq \omega_i \leq 838\ \mathrm{rad/s}, \quad i = 1, 2, \cdots, 6. \quad (27)$$

Two relevant experiments are now presented. In the first experiment the UGV moves in a straight line, while in the second the UGV moves along a curved trajectory, there is no communication between UGV and UAV, the whole landing approach is based only on internal UAV sensors with the absence of simulated GPS or simulated external localization system.

A. Linear UGV motion

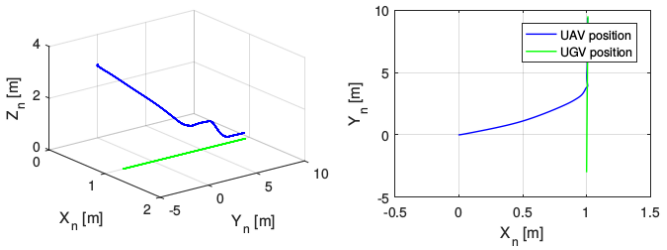

Fig. 6. Landing simulation result for the **linear** UGV motion. Left: 3D trajectory followed by the UAV and UGV. Right: 2D trajectory on the XY plane.

Figures 6 and 7 illustrate the result of a landing test when the UGV is moving with a linear trajectory. The landing process lasted near 13.5 seconds. At time $t = 2.5\,\mathrm{s}$, the motors are ignited and at $t = 3.5\,\mathrm{s}$, the land preparation mode was

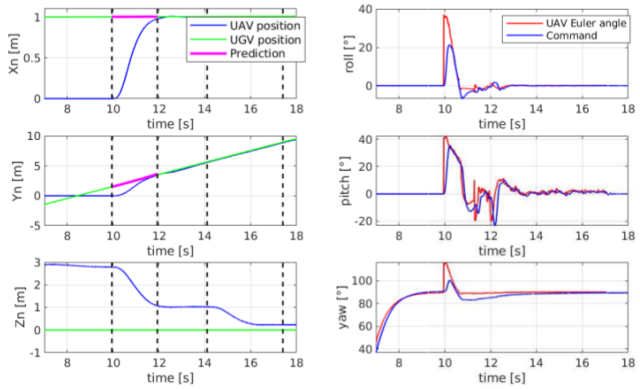

Fig. 7. Positions and angles during the landing manuever for the **linear** UGV motion, including the prediction of the UGV motion.

activated. At about $t = 7\,\mathrm{s}$, the UGV entered the FOV of the UAV and at $t = 10\,\mathrm{s}$ the UAV predicted a trajectory of the UGV, which is presented as purple lines in figure 7. Then the trajectory tracking mode was activated, and during this mode, the UGV gets lost from the FOV due to the large tilt angle needed to move the UAV forward. At $t = 13\,\mathrm{s}$, the UGV reappeared in the FOV and the UAV was then switched into approaching mode, it then tracks the UGV fully using the onboard camera. Finally, at $t = 14.5\,\mathrm{s}$, the UAV was almost right above the UGV and the docking mode was activated until $t = 17\,\mathrm{s}$ when the UAV has completed the landing process and the motors were shut down.

B. Curved UGV motion

Figures 8 and 9 illustrate the result of landing test with UGV moving along a circular trajectory. The steps followed by the state machine are similar to the previous test. In this case, the aim is to show that the system is capable to perform the landing also in different to linear UGV motions patterns. As can be seen in the figures, the successful landing process also lasted around 13 seconds.

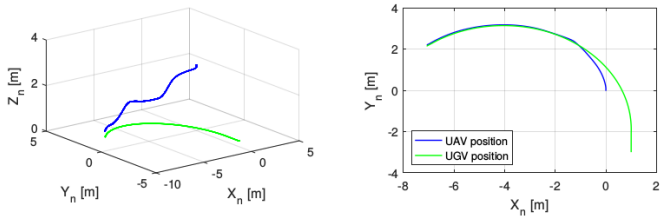

Fig. 8. Landing simulation result for the **circular** UGV motion. Left: 3D trajectory followed by the UAV and UGV. Right: 2D trajectory on the XY plane.

We simulated the previously described scenarios for three different maximum UGV velocities V_{max}: $1\,\mathrm{m/s}$, $1.5\,\mathrm{m/s}$ and $2\,\mathrm{m/s}$. For each V_{max}, 20 landings were simulated using a linear movement and 20 more using a curved motion of the UGV, with and without using prediction. The success rate sr and mean duration dt of the landings are presented in Table I.

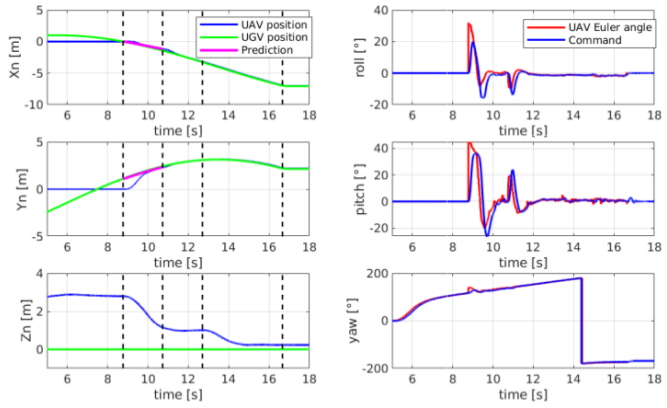

Fig. 9. Positions and angles during the landing manuever for the **circular** UGV motion, including the prediction of the UGV motion.

TABLE I
SUMMARY OF LANDING SUCCESS RATE.

		No prediction		With Prediction	
Type	V_{max} (m/s)	sr (%)	dt (m/s)	sr (%)	dt (m/s)
Linear	1	100	6.946	100	5.634
	1.5	80	11.213	100	9.421
	2	35	16.029	20	17.792
Curved	1	95	8.692	100	8.316
	1.5	90	16.739	100	10.375
	2	45	18.827	20	17.428

C. Discussion

The cubic spline trajectory (basic approach) enabled a smooth tracking of the multicopter UAV and performed decently at low speeds; however, the performance decreases for higher speeds. If the target UGV moves too fast, the cubic spline trajectory could lead to a velocity mismatch when the UAV arrives at the position of the target and the UAV may not be able to follow the target. This is why in Table I the results for the $1.5\,\mathrm{m/s}$ and $2\,\mathrm{m/s}$ velocities are the worst when no prediction is used. In terms of the duration of the landing maneuver, the higher the UGV speed the longer the duration, and linear movements have lower durations than curved ones.

On the other hand, by using trajectory prediction (our improved approach) we achieved a $100\,\%$ success rate on the low speeds for all types of motion and the performance decreases only on the highest speed. If the UGV moves too fast across the FOV, the UAV may not have enough time to acquire the necessary samples for a reliable prediction. This may be solved by using a different prediction scheme that requires fewer samples or by using a camera with a higher frame rate. In terms of duration, the trajectory prediction approach was faster than the basic approach in all cases.

VII. Conclusion and Outlook

A vision-based control system for UAV landing on a moving platform is presented, this system is able to successfully land the UAV even without GPS, external localization systems or a camera gimbal. The proposed system was implemented in ROS and tested intensively in the Gazebo simulator. An overall design solution was proposed for the autonomous landing mission, which included all steps from the initial state where the target is found by the UAV until it lands on the target platform successfully. A trajectory prediction system was designed, which provides an effective solution in case the target get lost from the FOV during agile multicopter movements.

Landing tests were performed with different UGV types of movements and velocities, and a comparison was made between a regular setpoint tracker and a trajectory tracking based on the movement prediction of the UGV. The results confirm that this design enables the UAV to reach the target set-point even when the target is lost from the FOV during the approach. As a consequence, the success rate of the landing maneuver was increased and the total landing time was reduced.

The validity of the proposed system was demonstrated; however only on low velocities. In the future, an algorithm based on an optimization approach could be implemented for the multicopter stabilization control, which should focus on stabilizing the plant with system feasibility constraints, such as linear quadratic regulator and model predictive control. The motion predictor should be replaced by one that requires fewer observed samples in order to achieve higher UGV velocities. Our next step is to test this approach in the real platform.

References

[1] A. Mendes, "Vision-based automatic landing of a quadrotor uav on a floating platform: A new approach using incremental backstepping," Ph.D. dissertation, TU Delft, Delft University of Technology, 2012.

[2] K. E. Wenzel, A. Masselli, and A. Zell, "Automatic take off, tracking and landing of a miniature uav on a moving carrier vehicle," *Journal of intelligent & robotic systems*, vol. 61, no. 1-4, pp. 221–238, 2011.

[3] Z. Zuo, "Trajectory tracking control design with command-filtered compensation for a quadrotor," *IET Control Theory & Applications*, vol. 4, no. 11, pp. 2343–2355, 2010.

[4] Z. Ceren and E. Altu, "Vision-based servo control of a quadrotor air vehicle," in *Computational Intelligence in Robotics and Automation (CIRA), 2009 IEEE International Symposium on*. IEEE, 2009, pp. 84–89.

[5] A. Chamseddine, Y. Zhang, C. A. Rabbath, C. Join, and D. Theilliol, "Flatness-based trajectory planning/replanning for a quadrotor unmanned aerial vehicle," *IEEE Transactions on Aerospace and Electronic Systems*, vol. 48, no. 4, pp. 2832–2848, 2012.

[6] D. Mellinger, M. Shomin, and V. Kumar, "Control of quadrotors for robust perching and landing," in *Proceedings of the International Powered Lift Conference*, 2010, pp. 205–225.

[7] K. Dalamagkidis, S. Ioannou, K. Valavanis, and E. Stefanakos, "A mobile landing platform for miniature vertical take-off and landing vehicles," in *2006 14th Mediterranean Conference on Control and Automation*. IEEE, 2006, pp. 1–6.

[8] A. Borowczyk, D.-T. Nguyen, A. P.-V. Nguyen, D. Q. Nguyen, D. Saussié, and J. L. Ny, "Autonomous Landing of a Multirotor Micro Air Vehicle on a High Velocity Ground Vehicle," *20th IFAC World Congress*, vol. 50, no. 1, pp. 10 488–10 494, 2017.

[9] M. Wierema, "Design, implementation and flight test of indoor navigation and control system for a quadrotor uav," *Master of Science in Aerospace Engineering at Delft University of Technology*, 2008.

[10] "AscTec Firefly wiki," http://www.asctec.de/en/uav-uas-drones-rpas-roav/asctec-firefly/l, 2016.

[11] R. Polvara, S. Sharma, J. Wan, A. Manning, and R. Sutton, "Towards autonomous landing on a moving vessel through fiducial markers," in *Mobile Robots (ECMR), 2017 European Conference on*. IEEE, 2017, pp. 1–6.

[12] J. S. Goddard and M. A. Abidi, "Pose and motion estimation using dual quaternion-based extended kalman filtering," in *Three-Dimensional Image Capture and Applications*, vol. 3313. International Society for Optics and Photonics, 1998, pp. 189–201.

[13] M. Euston, P. Coote, R. Mahony, J. Kim, and T. Hamel, "A complementary filter for attitude estimation of a fixed-wing uav," in *Intelligent Robots and Systems, 2008. IROS 2008. IEEE/RSJ International Conference on*. IEEE, 2008, pp. 340–345.

[14] J. Farrell, M. Polycarpou, and M. Sharma, "On-line approximation based control of uncertain nonlinear systems with magnitude, rate and bandwidth constraints on the states and actuators," in *American Control Conference, 2004. Proceedings of the 2004*, vol. 3. IEEE, 2004, pp. 2557–2562.